

PROPOSAL OF BENCHMARK PROBLEM OF THERMAL STRIPING PHENOMENA IN PLANAR TRIPLE PARALLEL JETS TESTS FOR FUNDAMENTAL CODE VALIDATION IN SODIUM-COOLED FAST REACTOR DEVELOPMENT

J. Kobayashi

Fast Reactor Technology Development Department,
Japan Atomic Energy Agency,
4002 Narita-cho, O-arai, Ibaraki 311-393, Japan
kobayashi.jun41@jaea.go.jp

M. Tanaka, S. Ohno and H. Ohshima

Fast Reactor Computational Engineering Department
Japan Atomic Energy Agency
4002 Narita-cho, O-arai, Ibaraki 311-393, Japan

H. Kamide

Advanced Fast Reactor Cycle System Research and Development Center,
Japan Atomic Energy Agency
4002 Narita-cho, O-arai, Ibaraki 311-393, Japan

ABSTRACT

Numerical simulation is recognized as an essential tool for the physical phenomena analysis and plant design study of sodium-cooled fast reactors (SFRs). In order to enhance credibility of the numerical results in the activities for plant design by using numerical simulations, it is recognized that verification and validation (V&V) process is very important. In this study, experiments for planar triple parallel jets mixing phenomena conducted in JAEA were proposed as benchmark problems for the code validation in the area of thermal striping study in SFR development. In the experiment, triple jets were simulating a control rod channel and two fuel assemblies on both sides of the channel because thermal striping can be caused in the region where the temperature fluctuation is induced by mixing of fluids at different temperatures. Since high cycle thermal fatigue in structure may be caused by thermal striping, investigation of mixing process of the jets and attenuation process of the temperature fluctuation from fluid to structure is highly required. The sodium experiment PLAJEST and the water experiment WAJECO were selected as the benchmark problem. A cold jet and two hot jets flow out vertically from the center nozzle and the neighbor nozzles. In a typical boundary condition at 0.5 m/s in axial velocity through the nozzle of 0.02 m in width, the Reynolds numbers were 2.8×10^4 and 1.5×10^4 at 348 °C in PLAJEST and at 40 °C in WAJECO, respectively. In the both experiments, the mixing area was located between the two parallel vertical walls and a metal test plate made of the stainless steel No.316 (SS316) with thermocouples in it was set on one side in order to investigate the transfer characteristics of temperature fluctuations from fluid to structure.

KEYWORDS

Thermal striping, Benchmark problem, Code Validation, Numerical simulation,
Sodium-cooled fast reactor.

1. INTRODUCTION

Temperature fluctuation can be induced in the region where hot and cold fluids are mixed and it may cause high cycle thermal fatigue in structural components. These phenomena are known as thermal striping. Thermal striping in liquid metal cooled fast reactors was recognized in the early 1980s by Wood [1] and Brunings [2], and has subsequently been studied by Betts [3] and Moriya [4]. For mixing phenomena in thermal striping, Tenchine [5, 6] investigated the mixing behavior of co-axial jets of sodium experiments and air jets experiments.

A series of water experiments called as WAJECO- I (1996~2000) for the triple-parallel jets mixing phenomena had been conducted by Tokuhiro [7-9] and Kimura [10, 11] to investigate the thermal mixing process among the jets. In WAJECO-I, water jets were formed through the straight-type nozzles in upstream of the test section [11]. In WAJECO-II (2000~2001) [12], metal plate was installed into the test section of WAJECO-I at the middle of the test section in parallel to the walls to investigate the thermal interaction between the fluid and the structure. The straight nozzle in the former test section was modified to the converged nozzle in WAJECO-III (2001~2003) [13] as shown in Fig. 1, without the center plate installed in the WAJECO-II. In WAJECO-IV (2003~2005) [14] as the latest test section dealt with in this paper, the attenuation process of the temperature fluctuation from fluid to structure was investigated with the test section. In the test section of WAJECO-IV, converged nozzle was used and a metal plate of stainless steel No. 316 (SS316) was installed on the wall.

Kimura [15-18] performed a sodium experiment called as PLAJECT (2001~2005) as shown in Fig. 1 that had triple-parallel jets along a stainless steel wall and showed that the transfer characteristics of temperature fluctuation from fluid to structure could be evaluated by using a heat transfer coefficient obtained from a transfer function between temperature fluctuations in fluid and structure. Furthermore in the sodium experiment PLAJECT, the configuration of the test section is almost the same with that in the water experiment WAJECO-IV. A stainless steel plate (SS316) with thermocouples was set along flow in order to evaluate the characteristics of temperature fluctuation transfer from fluid to structure compared with that in the water experiment of WAJECO-IV [14].

2. OUTLINE OF EXPERIMENTS

2.1 Test Section

The water experiment is called WAJECO (in this paper, indicating WAJECO-IV) and the sodium experiment is called PLAJECT [15-18]. The configuration of the test sections in both experiments are almost the same. Figure 1 shows the schematic view of the test section of both experiments. The x axis corresponds to normal (depth) direction to the vertical wall, the y axis is horizontal direction and the z

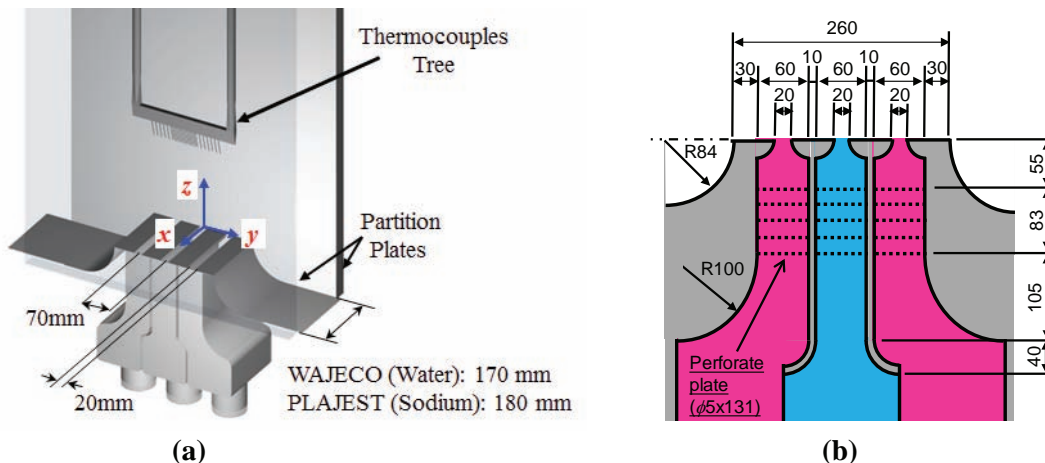


Fig. 1 Viewgraphs of (a) overview of the test section and (b) configuration of converged nozzles.

axis is vertical direction. The origin is set at the center of the cold jet on the nozzle outlet and on the wall surface.

Figure 2 shows the outline of the experimental apparatus of the sodium experiment PLAJEST. In the test section, a rectangular metal block with slope shape on both sides is installed in the bottom of the test section; it has three discharged nozzle outlets on the top surface. The height of the block is 85 mm from the bottom of the test section. Each nozzle outlet has rectangular cross section. Width in the horizontal direction is 20 mm and nozzle length in depth direction is 180 mm in PLAJEST, compared to 170 mm in WAJECO. In the benchmark, 180 mm in PLAJEST is the reference. A jet at low temperature flows out vertically from the center nozzle and the two jets at high temperature flow out vertically from the nozzle outlets on both sides of the center. Each nozzle has a rectangular duct on upstream side. In the upstream duct of each nozzle, six porous plates and a quadrant reducer are installed. The parallel walls are installed on both sides in the depth direction of the nozzle block. The test section is put between two vertical walls (plates). A metal test plate made of stainless steel type 316 (SS316) is installed in one side wall to investigate temperature fluctuation in the structure.

In WAJECO, the maximum flow rate in the hot flow line is 30 m³/h and that of in the cold flow line is 22 m³/h. The flow rate were measured using the electromagnetic flow meter (EMF) and the errors of the hot flow line and cold flow line flowrate correspond to 0.06 m/s and 0.09 m/s, respectively.

In PLAJEST, the flowmeters were calibrated by measuring volume of the fluid flowing through the meter and a time interval under approximately steady conditions of flow. The measurement errors of the flowmeters were estimated to be within 0.004 m/s at the outlet of nozzle.

2.2 Temperature Measurement

Figures 3(a) and (b) show the front and the side views of thermocouples-tree in the sodium experiment PLAJEST. In the thermocouples-tree, each thermocouple is installed in a stainless steel tube of 1.0 mm in diameter and the 5 mm long part of the thermocouple from the tip is exposed to the flow. In PLAJEST as shown in Fig. 3(a), fluid temperatures at 90 mm, 40 mm, 10 mm and 0.5 mm from the wall

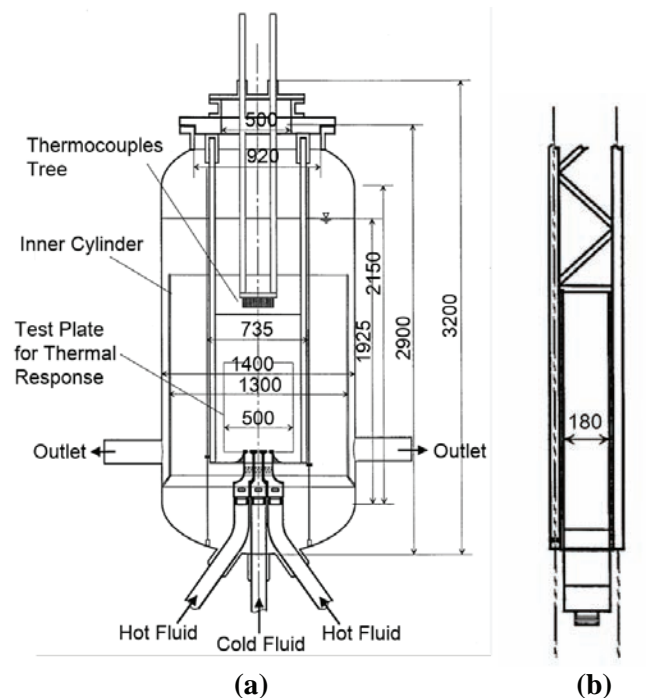


Fig. 2 Outline of experimental apparatus in sodium experiment PLAJEST in (a) view on the vertical cross section and (b) side view.

surface are measured by a movable thermocouples-tree. The thermocouples in the tree are non-contact K-type. Thermocouples of 0.3 mm in diameter are in the center part and of 0.5 mm in diameter are in the regions on both sides of the tree. The estimated measurement error is 0.1 °C by the relative calibration carried out at four levels from 250 °C to 400 °C. The time interval of the temperature measurement is 0.01 s and the number of the sampling temperature data at each position is 20,000 (total of 200 s).

In the water experiment WAJECO, the same thermocouples-tree is used [14]. In the movable thermocouples-tree, 39 thermocouples are installed with space of 5 mm between the neighbors. The thermocouples in the tree are non-contact K-type and the diameter of the thermocouple is 0.25 mm. The response time constant of the thermocouple is approximately 5.7 ms. The estimated measurement error is 0.1°C by the relative calibration test. The time interval of the temperature measurement is 0.01 s and the number of temperature data collected at each position is 4200 (total of 42 s) in the water experiment.

Metal plate made of SS316 with thermocouples is installed in a part of the partition wall exposed to the mixing region of the jets in PLAJECT. Dimensions of the SS316 plate are 12 mm in depth (*x*) direction as the plate thickness, 500 mm in horizontal direction (*y*) and 600 mm in vertical direction (*z*) from the level of the nozzle outlet. As shown in Fig. 3, thermocouples of 0.5 mm in diameter are installed in the plate at 0.25 mm (26 point), 1.5 mm (14 points), 2 mm (5 points) and 11.75 mm (5 points) from surface. The sampling interval of temperatures was 0.1 s and the number of the data was 20,000 (total of 200 s).

2.3 Velocity Measurement in Water Experiment (WAJECO)

The Particle Image Velocimetry (PIV) technique is used to measure velocity field in the mixing area. A laser sheet, generated by a double-pulsed Nd-YAG laser system, is inserted into the test section. Small particles made of Nylon are used as tracer and the diameter of the particles is approximately 30~50 μm. The CCD camera which can capture 60 images per second is set in front of the test section. The pixel numbers of one image are 640 in horizontal direction and 480 in vertical direction, and the size of the picture image was 40 mm and 30 mm. The spatial resolution of velocity measurement is 1.3 mm. The time interval between two images is 1 ms. Since the picture size is limited, a number of images are captured to cover the whole part of the test section by moving the CCD camera and the laser sheet. The velocity field in the horizontal half region of the test section from the cold jet to the right hot jet is

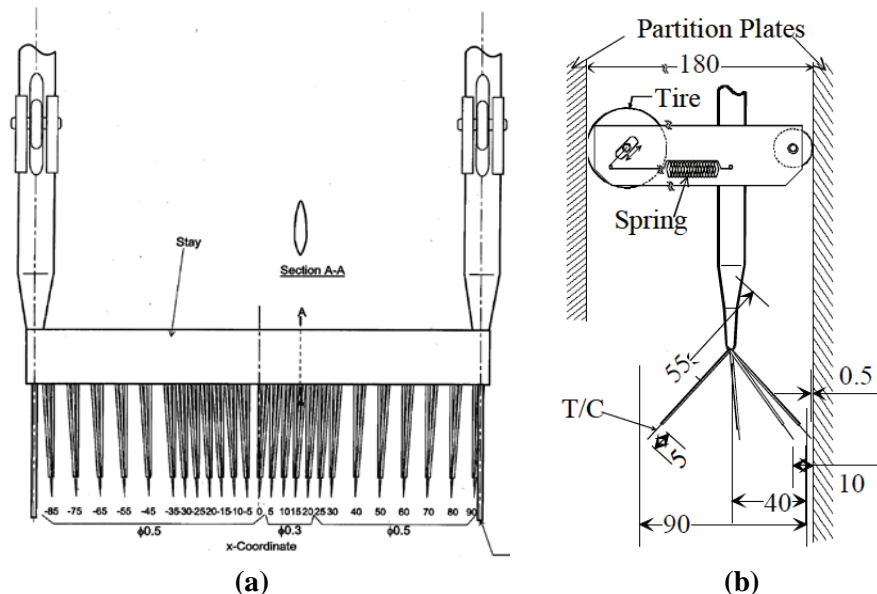


Fig.3 Thermocouples-tree arrangement at (a) front view and (b) side view in the sodium experiment PLAJECT.

measured. The time interval of the velocity measurement was 0.033s and the number of the data was 180 (=6 s) at each position. The images were captured in three times at the same position to increase the number of data for statistical analysis. The total number of velocity data was 540 per one measured point. As mentioned above, configuration of the test section of WAJECO is the almost same with that of PLAJECT. Velocity profiles in WAJECO can, therefore, be extrapolated to those in PLAJECT.

2.4 Experimental Conditions

It may be assumed that flow field in sodium experiment is similar to that in water experiment if a buoyancy force is negligible, because the viscosity of liquid sodium is the same order of that of water in comparison of the properties of liquid sodium and water. Since sodium has a very large thermal conductivity in comparison with that of water, on the other hand, temperature distribution of the sodium test may be different from that of the water test. Therefore, sodium and water tests must be conducted comparably with the same test section in configuration. Moreover, the thermal conductivity of the structure is an important factor to evaluate the decay characteristics of temperature fluctuation. Material of the metal plate in both experiments is stainless steel SS316. Table 2 shows typical experimental conditions as candidates for the benchmark problem. The Reynolds number is defined as follows:

$$Re = \frac{V_m D}{\nu} \quad (1)$$

$$V_m = \frac{V_c + 2V_h}{3} \quad (2)$$

D is the nozzle width (=20 mm) and V_m is the mean discharged velocity of the three jets. V_c is the mean velocity of the cold jet from the center nozzle and V_h is the mean velocity of the hot jets from the nozzles on both sides of the center one. The temperature difference ΔT at discharged nozzle is simply defined as follows:

$$\Delta T = T_h - T_c \quad (3)$$

T_h and T_c are time average temperatures at the nozzle of the hot and cold jets, respectively. Estimated mixed-mean temperature T_m is defined as follows:

$$T_m = \frac{V_c T_c + 2V_h T_h}{3V_m} \quad (4)$$

3. CANDIDATE CASES FOR BENCHMARK SIMULATION

3.1 Candidate cases

Benchmark simulation cases are to be chosen from the experimental conditions in the sodium experiment PLAJECT. There are two typical experimental cases as shown in Table 1.

One is the isovelocity case (Case-A1 and Case-A2 in Table-2) in which a characteristic dominant frequency was observed in the fluid temperature fluctuation around the center jet in the mixing region. To know relation between such a characteristic temperature fluctuation generation mechanism and the mixing behavior is important, Case-A1 for PLAJECT with stainless steel plate is selected as a primary case in the benchmark problem. In PLAJECT, no information of the velocity field was obtained. The configuration of test sections of WAJECO and PLAJECT are almost the same. A simulation of Case-A2 for WAJECO at the same velocity conditions in PLAJECT is employed so as to compare the velocity

profile obtained in WAJECO with the numerical results. Both simulations of Case-A1 and Case-A2 can be conducted with the same computational domain. Therefore, Case-A1 for PLAJECT and Case-A2 for WAJECO with stainless steel plate as an isovelocity condition may be taken in benchmark problem.

On the other hand, a hetero-velocity condition Case-B1 for PLAJECT can be selected as the case for the benchmark. Since shear stress is caused between the center jet and both side jets, the flow pattern (eddy structure) in the mixing region and the temperature fluctuation generation mechanism may be different from those in the isovelocity case Case-A1. The benchmark simulations of Case-A1, Case-A2, and Case-B1 may be helpful in understanding temperature fluctuation generation mechanism, in triple jet mixing configuration through the benchmark problem.

3.2 Dimensions of Recommended Computational Domain

Figure 4 shows recommended computational domains of 192 mm (=180 mm + 12 mm) in depth, 500 mm (25D) in horizontal direction and 685 mm (=600 mm + 85 mm) in vertical direction from the bottom of the test section, as the minimum size for the benchmark. In Fig. 4, converged nozzles on upstream as shown in Fig. 1 (b) are modeled. The recommended computational domain for the benchmark is established through the following considerations. For the width in horizontal direction, at least, 430 mm consisting of 260 mm as a width of the top surface of the nozzle block and 170 mm (= 2 × 85 mm) as length of the slopes on both sides of the block is needed. For the height in vertical direction, a distance of more than 20D is needed based on the time average temperature profile along the vertical direction in the water experiment of WAJECO [14]. 600 mm (=30D) in vertical from the level of the nozzle outlet is recommended. Although a symmetrical condition on the middle cross section between the walls can be assumed in the mixing region, consideration of the full distance of 180 mm (=L) between the walls and the thickness of 12 mm of the metal plate is recommended to analyze the three dimensional flow structures in the mixing region and the thermal interaction between the fluid and the structure.

3.3 Inlet Boundary Condition

Figures 5 (a) and (b) show horizontal distributions of the time average velocity and the axial velocity fluctuation intensity normalized by the mean velocity at 0.54 m/s at 0.1 mm from the nozzle exit obtained from the water experiment WAJECO by using the PIV technique [14, 18]. The axial velocity distribution near the nozzle exit shows the almost flat profile. Setup of the inlet boundary condition is optional. The most simplest way is to set the mean velocity on the nozzle exit without calculating the flow through the upstream converged nozzle or to set the velocity profiles proved in Figs. 5(a) and (b). If the upstream converged nozzles a shown in Fig. 1 (a) are modeled in the domain, flow patterns can be calculated.

3.4 Outlet Boundary Condition

In PLAJECT, the test section is installed in a cylindrical vessel within the sodium loop apparatus as

Table 1 Experimental Conditions for Benchmark Problem

Case	Outer-slits/Hot jets		Center-slit/Cold jet		Index of mixture		
	V_h (m/s)	T_h (°C)	V_c (m/s)	T_c (°C)	V_m (m/s)	ΔT (°C)	T_m (°C)
A1 (SJ3-A05)*1)	0.51	347.5	0.51	304.5	0.51	43	333.2
A2 (WJ4s-A01)*2)	0.48	40.3	0.48	32.0	0.48	8.3	37.5
B1 (SJ3-A11)*3)	0.51	349.8	0.32	311.0	0.45	38.8	340.5

*1) NUTHOS-7⁽¹⁷⁾ and NURETH-11⁽¹⁶⁾, *2) NURETH-12⁽¹⁴⁾, *3) NURETH-11⁽¹⁶⁾

shown in Fig. 2. In the vessel, a cylindrical inner wall is installed between the vessel and the test section. Sodium from the nozzles in the test section overflows into the narrow gap between the inner cylinder and the vessel. In the water experiment WAJECO, the test section is installed in rectangular vessel within the water loop apparatus and the water from the nozzles in the test section overflows into the gap between the test section and the rectangular vessel. In both experiments, horizontal flow to the gap may occur near the free surface on the top of the test section due to the overflows and weak recirculation flows from the side wall to the mixing region may be induced. To simulate the flows in the whole part of the test section precisely, very wide area should be considered as computational domain and a number of meshes are needed. Since side walls of the test section are far from the mixing region as shown in Fig. 2, the mixing region may not be affected by such induced flows in the test section. Then, a limited computational domain focusing on the mixing region as shown in Fig. 4 can be appropriate and outlet boundaries can be set around the domain. Previously, Kimura et al. [14, 17] set outlet boundaries on the top and the both side boundaries though a part of the side wall near upper corner of the computational domain is blocked to make stable outlet flow condition. Participants can arrange outlet boundary condition in the domain to make reasonable flow pattern in the test section.

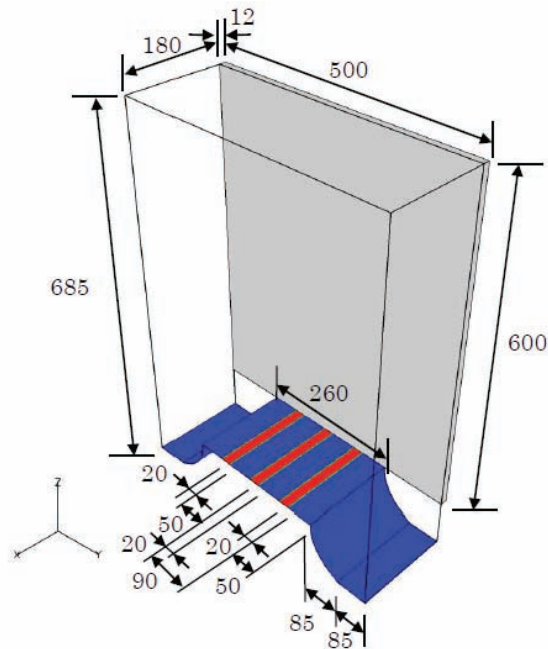


Fig. 4 Dimensions of a recommended computational domain.

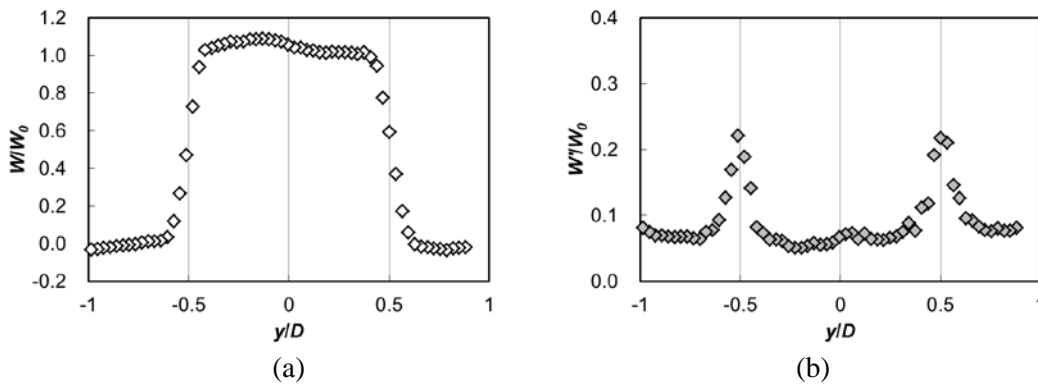


Fig. 5 Horizontal distributions of (a) time average velocity and (b) axial velocity fluctuation intensity at 0.1 mm from the nozzle exit in WAJECO.

3.5 Boundary Condition for Metal Plate

In Cases-A1 and B1 for PLAJECT and Case-A2 for WAJECO, the metal plate made of SS316 should be modeled in the domain. Adiabatic condition may be set on the top, the bottom and the both side walls. The mixed-mean temperature T_m that is the bulk temperature in the vessel in Table 1 may be applied on the back side wall and the thermal interaction between the fluid and the plate should be considered in the simulation.

Table 2 List of provided data for benchmark exercise.

Provided data	Case	x/D		Figure
Horizontal distribution of time average horizontal velocity component		4.25		Fig. 6 (a-1)
		0.05		Fig. 6 (a-2)
Horizontal distribution of fluctuation intensity of horizontal velocity component		4.25		Fig. 6 (b-1)
		0.05		Fig. 6 (b-2)
Horizontal distribution of time average vertical velocity component	A2	4.25		Fig. 7 (a-1)
		0.05		Fig. 7 (a-2)
Horizontal distribution of fluctuation intensity of vertical velocity component		4.25		Fig. 7 (b-1)
		0.05		Fig. 7 (b-2)
Horizontal distribution of time average temperature at the middle of the test section	A1	4.5	$y/D = -5.0 \sim 5.0$ and $z/D=5.0$	Fig. 8 (a-1)
	B1			Fig. 8 (a-2)
	A2			Fig. 8 (a-3)
Horizontal distribution of temperature fluctuation intensity at the middle of the test section	A1	4.5		Fig. 8 (b-1)
	B1			Fig. 8 (b-2)
	A2			Fig. 8 (b-3)
Horizontal distribution of time average temperature at the near wall location	A1	0.025		Fig. 9 (a-1)
	B1			Fig. 9 (a-2)
	A2			Fig. 9 (a-3)
Horizontal distribution of temperature fluctuation intensity at the near wall location	A1	0.025		Fig. 9 (b-1)
	B1			Fig. 9 (b-2)
	A2			Fig. 9 (b-3)
Temperature fluctuation intensity from fluid to structure	A1	4.5 ~ -0.6		Fig. 10 (b)
	A2	4.25 ~ 0.0		Fig. 10 (c)
PSD profiles of temperature fluctuation intensity from fluid to structure at Case-A1	A1	4.5	$y/D = 0.75$ and $z/D=5.0$	Fig. 11 (a)
		0.025		Fig. 11 (b)
		-0.0125		Fig. 11 (c)
PSD profiles of temperature fluctuation intensity from fluid to structure at Case-A2	A2	4.5		Fig. 12 (a)
		0.025		Fig. 12 (b)
		-0.00625		Fig. 12 (c)

4. EXPERIMENTAL RESULTS

4.1 Experimental Data for Comparison

The provided data for comparisons are listed in Table 2. For the temperature, the profiles of time-average and fluctuation intensity on vertical, horizontal and depth directions and the power spectrum density (PSD) of temperature fluctuation analyzed by the Fast Fourier Transform (FFT) method at typical positions in fluid and structure are provided. For the velocity components, horizontal distributions of time-average and fluctuation intensity of the horizontal and the vertical velocity components are provided. Provided data are related to the location at $y = -15$ mm ($y/D = -0.75$) and $z = 100$ mm ($z/D=5$) between the center jet and the side jet where the maximum temperature fluctuation intensity is observed. Provided horizontal distributions of fluid temperature and velocity from $y/D = -5$ to $y/D = 5$ shows the phenomena in the area where the dominant mixing phenomena occur.

4.2 Velocity Distributions above the Nozzle Exit

Figure 6 shows the horizontal distributions of (a) the time average and (b) the fluctuation intensity of the horizontal velocity component at (1) $x/D = 4.25$ and (2) $x/D = 0.05$ from the wall surface at $z/D = 5$, respectively. Horizontal profiles from $y/D = -5$ to $y/D = 5$ are shown. The positive horizontal velocities were shown in the negative locations in y/D axis and the negative velocities were shown in the positive locations in y/D axis. This indicates that the outer jets leaned to the center jet. And velocity fluctuation intensity was high at both boundaries between the center jet and the neighbor outer jets. In comparison to the results as shown in Figs. 6 (b-1) and (b-2), the magnitude of the velocity fluctuation intensity decreased near wall region in Fig. 6 (b-1) due to the influence of the wall.

Figure 7 shows the horizontal distributions of (a) the time-average and (b) the fluctuation intensity of axial velocity component at (1) $x/D = 4.25$ and (2) $x/D = 0.05$ from the wall surface at $z/D = 5$,

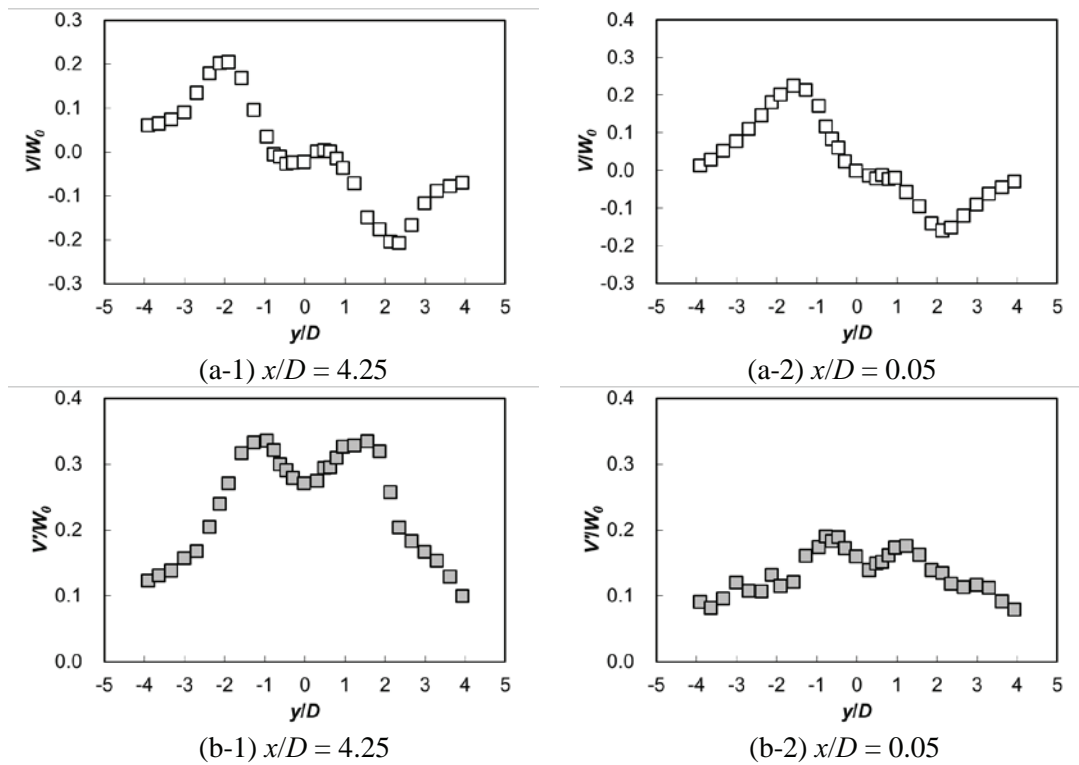


Fig. 6 Horizontal distributions of (a) time average and (b) fluctuation intensity of horizontal velocity component at (1) the middle and (2) the near wall locations.

respectively. Horizontal profiles from $y/D = -5$ to $y/D = 5$ are shown. Magnitude of the axial velocity at the center of the outer jets ($y/D \sim \pm 2$) was higher than that of the center jet, though the discharged velocities as inlet boundary condition was the same for each nozzle. On the contrary, axial velocity intensity in the center jet ($y/D = 0$) was higher than that in the outer jets. In comparisons with results shown in Figs. 7 (b-1) and (b-2), magnitude of the velocity fluctuation intensity decreased near wall region in Fig. 7 (b-1) due to the influence of the wall.

Thus, these measured results as shown in Figs. 6 and 7 include the important information on the mixing mechanism and they are suitable as the reference results for the benchmark problem.

4.3 Temperature distributions above the Nozzle Exit

Figure 8 shows the horizontal distributions of (a) time average and (b) fluctuation intensity of fluid temperature in (1) Case-A1, (2) Case-A2, and (3) Case-B1 at the middle position between the walls and at $z/D = 5$. The time average temperature distributions in Case-A1 (sodium) and Case-A2 (water) were similar to each other, though the temperature in Case-A1 was slightly lower than that in Case-A2 at the center of the cold jet. The temperature fluctuation intensity was high in the boundary region between the hot jets and the cold jet ($y/D \sim \pm 1.5$). In the case of the isovelocity condition, the region with the large temperature fluctuation intensity was observed at both boundary regions of the cold jet, symmetrically. In the anisovelocity condition of Case-B1 (sodium), on the other hand, the low temperature region at the center went to the left-side hot jet and the high temperature fluctuation intensity region was observed at one side of the cold jet, asymmetrical.

Figure 9 shows the horizontal distributions of (a) time average and (b) fluctuation intensity of fluid temperature in (1) Case-A1, (2) Case-A2, and (3) Case-B1 near the wall at $z/D = 5$. In the case of the isovelocity condition Case-A1 (sodium) and A2 (water), the profiles of the time average temperature in Case-A1 were similar to that in Case-A2, though the temperatures in Case-A1 were slightly larger than that in Case-A2 at the center of the cold jet, as the same results in the middle region as shown in Fig. 8.

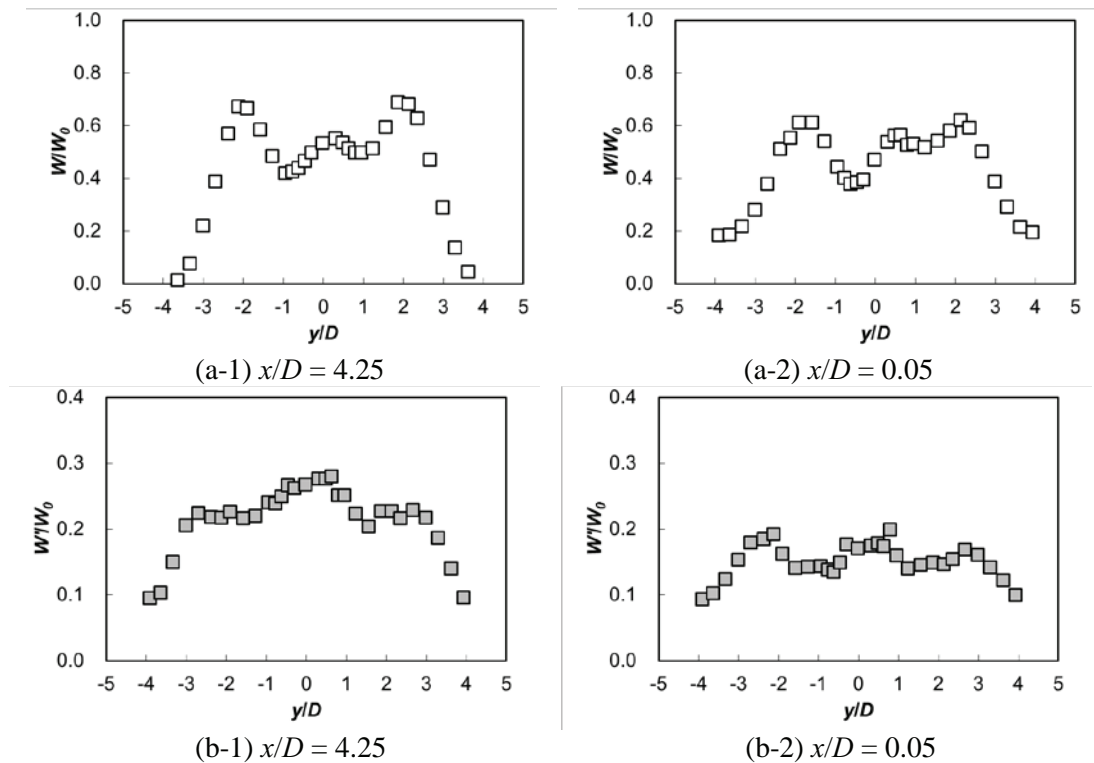


Fig. 7 Horizontal distributions of (a) time average and (b) fluctuation intensity of axial velocity component at (1) the middle and (2) the near wall locations.

Compared to the results at the middle position shown in Fig. 8, magnitude of the temperature fluctuation intensity decreased near wall region as shown in Fig. 9. The attenuation effect of the wall on the fluctuation intensity was also shown in the results of the velocity profiles as shown in Figs. 6 and 7.

In this point of view, the temperature behavior as shown in Figs. 8 and 9 are linked to the velocity field. These measured results of temperature as shown in Figs. 8 and 9 also include the important information on the mixing mechanism and they are suitable as the reference results for the benchmark problem.

4.4 Temperature Fluctuation Profiles from Fluid to Structure

Figure 10 shows the comparison of the decay characteristics of temperature fluctuation intensity from the mixing area far from the wall to the vicinity area of the wall surface between Case-A1 (sodium) and Case-A2 (water) at $y/D = -0.75$ and $z/D = 5$. The horizontal axis is the distance from the wall surface to the middle position in the mixing area, and the vertical axis is the normalized temperature fluctuation intensity. The temperature fluctuation intensity in the water experiment was similar to that in the sodium experiment at the center between the two partition plates. In the water experiment, the temperature fluctuation intensity increased once as the measured point approached to the wall. And then, the temperature fluctuation intensity decreased in the vicinity of the wall surface. Kimura [17] explained this profile due to the influence of the boundary layer from the wall. It is very much required for the benchmark exercise to clarify the attenuation mechanism of the temperature fluctuation intensity in the vicinity area of the wall by numerical simulations.

4.5 PSD profiles of Temperature Fluctuations

Figures 11 and 12 show the profiles of the power spectrum density (PSD) of the temperature fluctuation at representative locations from fluid to structure in Case-A1 (sodium) and Case-A2 (water),

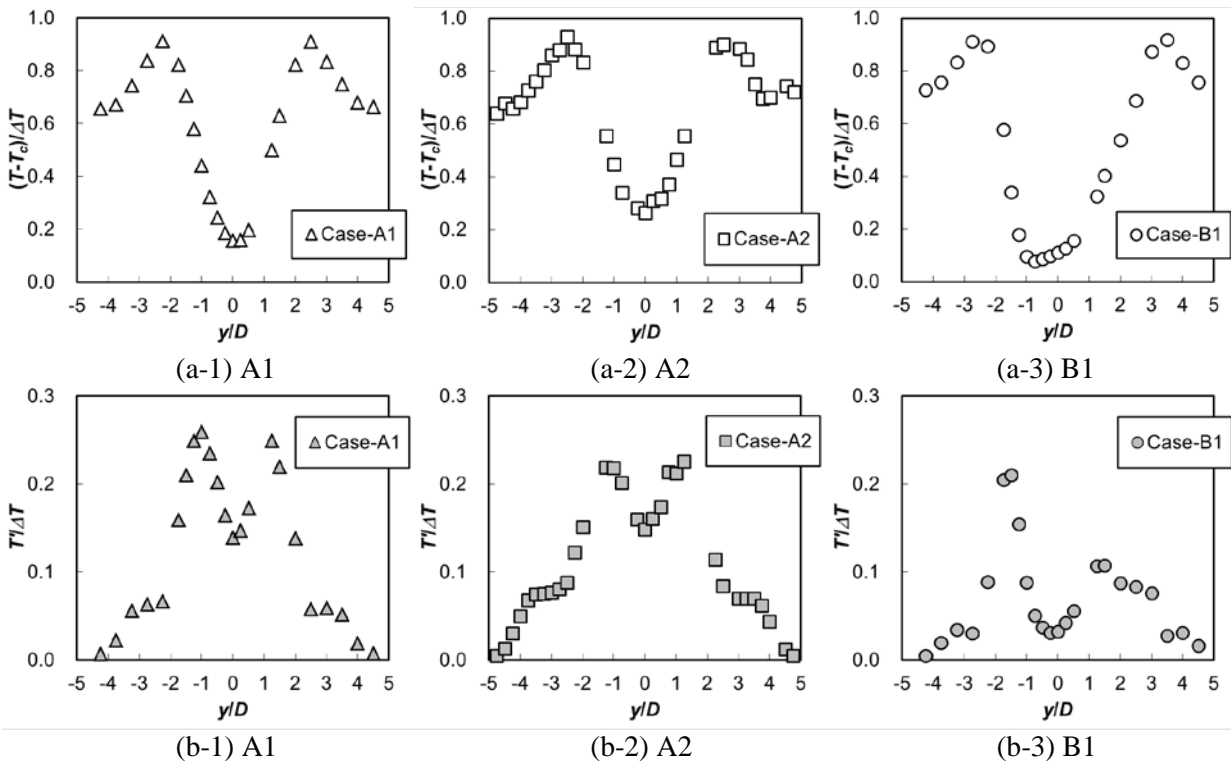


Fig. 8 Horizontal distributions of (a) time average and (b) fluctuation intensity of fluid temperature in (1) Case-A1, (2) Case-A2 and (3) Case-B1 at the middle between the walls and at $z/D = 5$.

respectively, at $y/D = -0.75$ and $z/D = 5$. The power spectrum density (PSD) was obtained at the position where maximum temperature fluctuation intensity was found in the cross section at the center between the two partition plates. The horizontal axis is the frequency components and the vertical axis is the power of temperature fluctuations normalized by the discharged temperature difference.

In the case of the isovelocity condition, the dominant frequency component was observed in all experiments. The dominant frequency component of temperature fluctuation was due to the jet oscillation. In the case of these isovelocity conditions of Case-A1 and Case-A2, the PSD profile in the water experiment shifted to the lower frequency side in comparison with that in the sodium experiment under the velocity similarity condition. The power in the dominant frequency in Case-A2 (water) was lower than that in Case-A1 (sodium). In Case-A2, the PSD in the low frequency region was relatively high comparing with that in Case-A1. In the vicinity of the wall surface, however, the PSD profile in Case-A2 shifted to the lower frequency side, comparing with that in Case-A1.

Kimura [14, 17] indicated that the water experiment could almost simulate the temperature

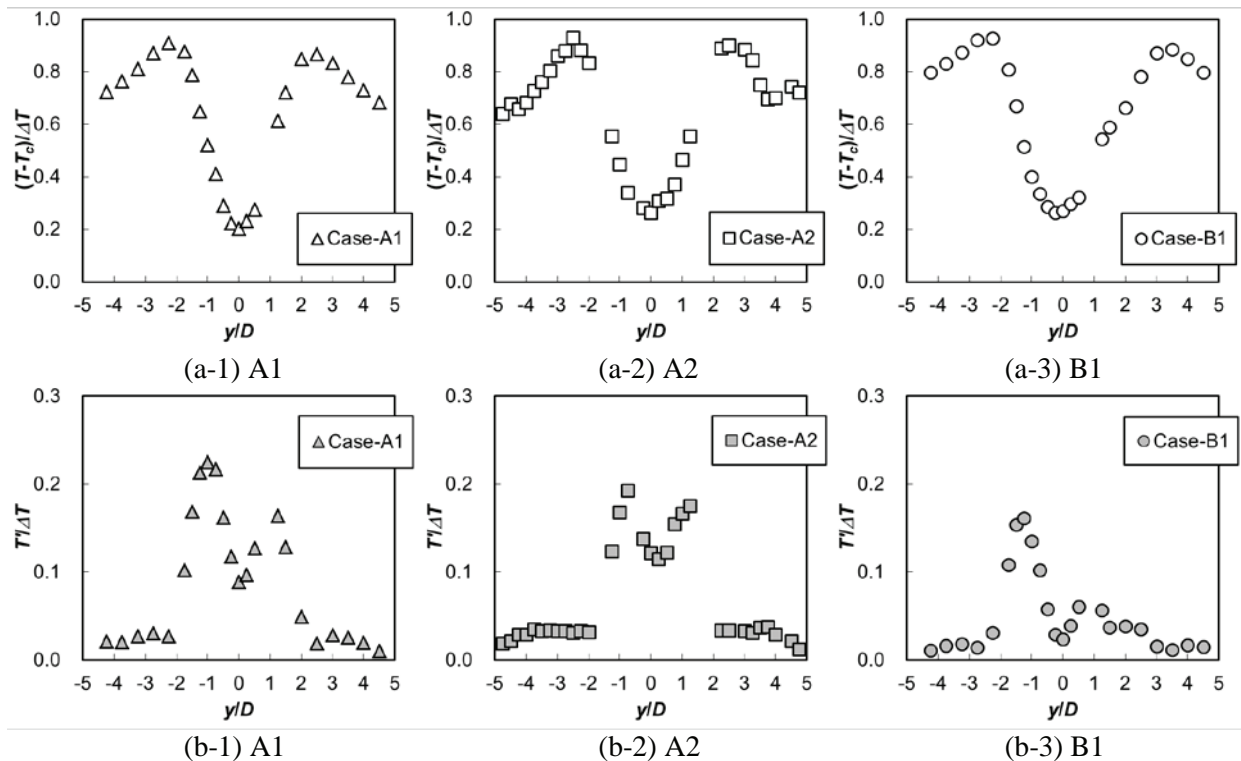


Fig. 9 Horizontal distributions of (a) time average and (b) fluctuation intensity of fluid temperature in (1) Case-A1, (2) Case-A2 and (3) Case-B1 near wall position at $z/D = 5$.

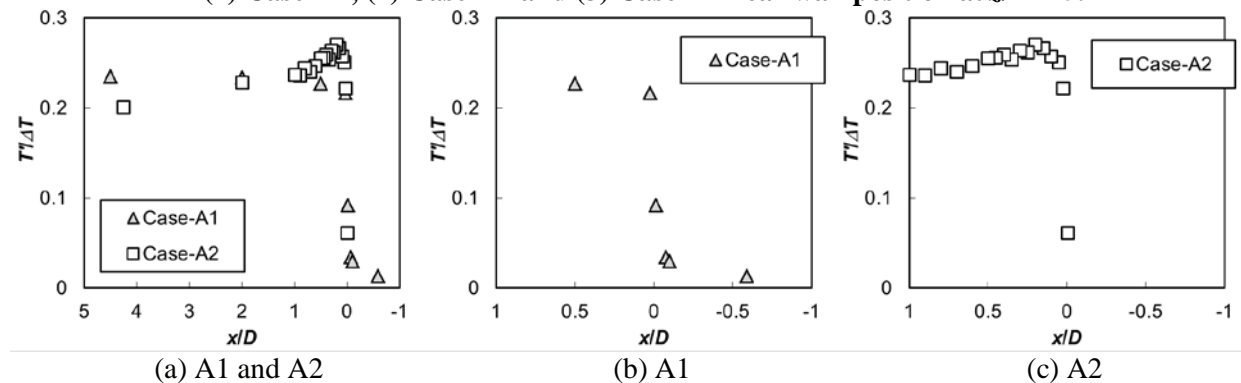


Fig. 10 Profiles of temperature fluctuation intensity from the mixing area far from the wall to the structure in Case-A1 (sodium) and Case-A2 (water) at $y/D = -0.75$ and $z/D = 5$.

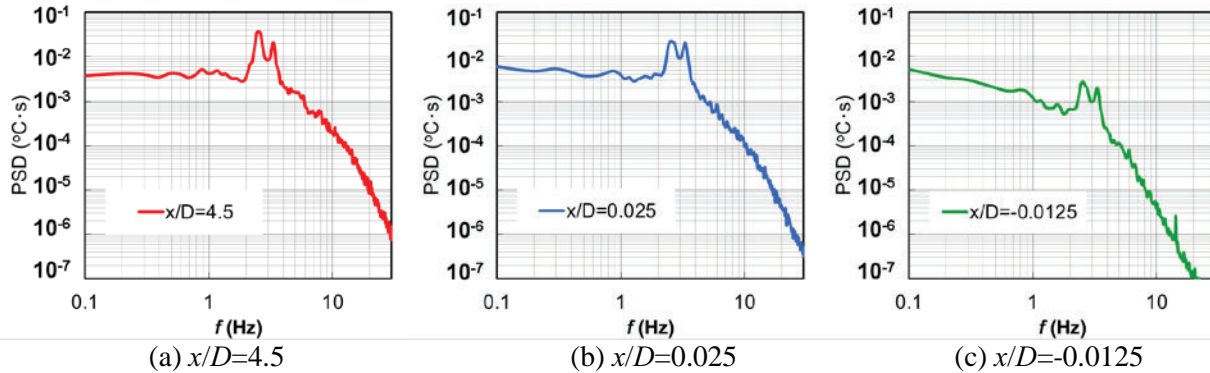


Fig. 11 Power spectrum density (PSD) of the temperature fluctuation at representative locations from fluid to structure in Case-A1 (sodium).

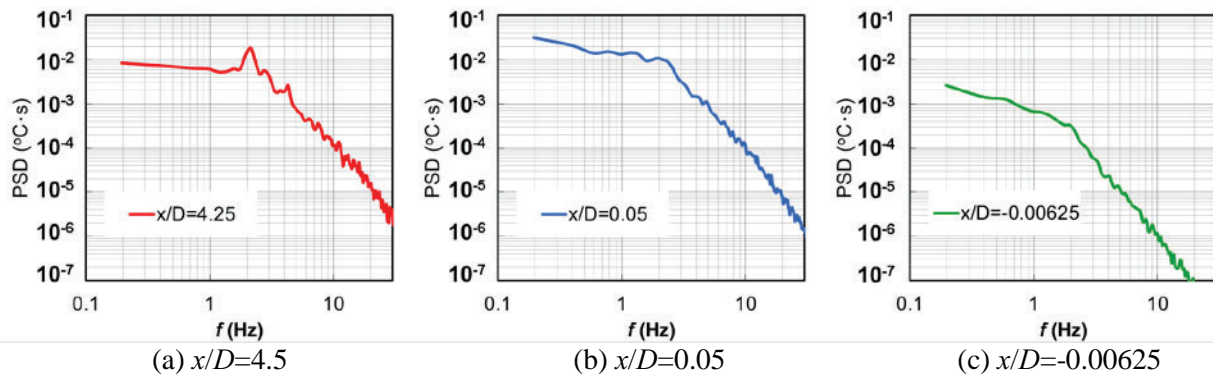


Fig. 12 Power spectrum density (PSD) of the temperature fluctuation at representative locations from fluid to structure in Case-A2 (water).

fluctuation in the sodium with respect to the frequency characteristics of temperature fluctuation in the vicinity of the wall surface conservatively.

5. CONCLUSIONS

Thermal striping phenomena may occur in a region where temperature fluctuations are induced by mixing of fluids at different temperatures. Water and sodium experiments, WAJECO and PLAJECT respectively, were conducted using planar triple parallel jets test apparatuses for investigating the attenuation process of the temperature fluctuation transfer from fluid to structure. The triple jets test section can simulate a control rod channel and two fuel assemblies on both sides of the channel. The results of WAJECO and PLAJECT were reviewed and experimental conditions for numerical benchmark problems were appropriately selected. Some recommendations of numerical analysis scheme and boundary conditions were proposed as benchmark problems for the code validation. It is believed that the results can be widely utilized for code validation.

REFERENCES

- (1) D. S. Wood, "Proposal for design against thermal striping", *Nuclear Energy*, **19**(6), pp.433-437 (1980).
- (2) J. E. Brunings, "LMFBR thermal-striping evaluation", Interim report, Research Project 1704-11, prepared by Rockwell International Energy Systems Group, EPRI-NP-2672 (1982).
- (3) C. Betts, C. Bourman and N. Sheriff, "Thermal striping in liquid metal cooled fast breeder reactors", *Proc. of NURETH-2*, Santa Barbara CA, USA, Vol. 2, pp.1292-1301 (1983).

- (4) S. Moriya, S. Ushijima, N. Tanaka, S. Adachi and I. Ohshima, "Prediction of Thermal Striping in Reactors", *Proc. of Int. Conf. Fast Reactors and Related Fuel Cycles*, Kyoto, Japan, Oct. 28–Nov. 1 1991, Vol. 1, pp.10.6.1-10.6.10 (1991)
- (5) D. Tenchine and J. P. Moro, "Experimental and numerical study of coaxial jets", *Proc. of NURETH-8*, Kyoto, Japan, Sept. 30 - Oct. 4, 1997, Vol. 3, pp.1381-1387 (1997).
- (6) D. Tenchine, S. Vandroux, V. Barthel and O. Cioni, "Experimental and numerical studies on mixing jets for sodium cooled fast reactor", *Nuclear Engineering and Design*, **263**, pp. 263-272 (2013).
- (7) A. Tokuhira, N. Kimura and H. Miyakoshi, "An experimental investigation on thermal striping. Part I: Mixing of a vertical jet with two buoyant heated jets as measured by ultrasound Doppler velocimetry", *Proc. of NURETH-8*, Kyoto, Japan, Sept. 30 - Oct. 4, 1997, Vol. 3, pp.1712-1723 (1997).
- (8) N. Kimura, A. Tokuhira and H. Miyakoshi, "An experimental investigation on thermal striping. Part II: Heat transfer and temperature measurement results", *Proc. of NURETH-8*, Kyoto, Japan, Sept. 30 - Oct. 4, 1997, Vol. 3, pp.1724-1734 (1997).
- (9) A. Tokuhira, N. Kimura, J. Kobayashi and H. Miyakoshi, "An investigation on convective mixing of two buoyant, quasi-planar jets with a non-buoyant jet in-between by ultrasound Doppler velocimetry", *Proc. of ICONE-6*, San Diego CA, USA, May 10-15, 1998, ICONE-6058 (1998).
- (10) A. Tokuhira and N. Kimura, "An experimental investigation on thermal striping. Mixing phenomena of a vertical non-buoyant jet with two adjacent buoyant jets as measured by ultrasound Doppler velocimetry", *Nuclear Engineering and Design*, **188**, pp.49-73 (1999).
- (11) N. Kimura, M. Nishimura and H. Kamide, "Study on Convective Mixing for Thermal Striping Phenomena (Experimental Analyses on Mixing Process in Parallel Triple-Jet and Comparisons between Numerical Methods)", *JSME International Journal (B)*, **45**(3), pp. 592-599, (2002).
- (12) N. Kimura, M. Igarashi and H. Kamide, "Investigation on Convective Mixing of Triple-jet - Evaluation of Turbulent Quantities using Particle Image Velocimetry and Direct Numerical Simulation -", *Proc. of the 8th International Symposium on Flow Modeling and Turbulence Measurements*, Tokyo, Japan, Dec. 4-6, 2001, pp. 651-658 (2001).
- (13) H. Kamide, N. Kimura, M. Igarashi and K. Hayashi, "Experimental Study on Temperature Fluctuation near Wall for Evaluation of Thermal Striping", *Proc. of NUTHOS-6*, Nara, Japan, Oct. 4-8, 2004, N6P347 (2004).
- (14) N. Kimura, H. Kamide, P. Emonot and K. Nagasawa, "Study on Thermal Striping Phenomena in Triple-Parallel Jet - Investigation on Non-Stationary Heat Transfer Characteristics Based on Numerical Simulation -", *Proc. of NURETH-12*, Pittsburgh PA, USA, Sept. 30-Oct. 4, 2007, Log Number: 117 (2007).
- (15) N. Kimura, H. Miyakoshi and H. Kamide, "Experimental Investigation on Transfer Characteristics of Temperature Fluctuation from Liquid Sodium to Wall in Parallel Triple-jet", *Int. J. Heat and Mass Transfer*, **50**, pp.2024-2036, 2007.
- (16) N. Kimura¹, H. Miyakoshi, H. Ogawa, H. Kamide, Y. Miyake and K. Nagasawa, "Study on Convective Mixing Phenomena in Parallel Triple-Jet along Wall - Comparison of Temperature Fluctuation Characteristics between Sodium and Water -", *Proc. of NURETH-11*, Avignon, France, Oct. 2-6, 2005, Paper: 427 (2005).
- (17) N. Kimura, H. Kamide, P. Emonot and K. Nagasawa, "Study on Thermal Striping Phenomena in Triple-Parallel Jet - Transfer Characteristics of Temperature Fluctuation in Sodium and Water based on Conjugated Numerical Simulation -", *Proc. of NUTHOS-7*, Seoul, Korea, October 5-9, 2008.
- (18) N. Kimura, H. Kamide and K. Nagasawa; P. Emonot, "Study on thermal-hydraulics of thermal striping phenomena; Evaluation of transfer characteristics of temperature fluctuation based on conjugated numerical simulation in triple-parallel jet geometry", JAEA Research 2012-017 (2012). (in Japanese)